

Supporting Information

Stretchable Triboelectric Nanogenerator with Exteroception- Visualized Multifunctionality

Qingyu Meng,^{†a} Minghao Zhang,^{†a} Ruixin Tang,^a Wenjing Jin,^a Jiayi Zhang,^a Zhuyue Lan,^a Shitao Shi,^a Xiaoping Shen,^{*a} and Qingfeng Sun^{*a}

^aCollege of Chemistry and Materials Engineering, Zhejiang A&F University, Hangzhou 311300, People's Republic of China

^{*}Corresponding authors: Xiaoping Shen, E-mail: xpshen@zafu.edu.cn; Qingfeng Sun, E-mail: qfsun@zafu.edu.cn

Materials and chemicals

HPC with an average MW of 33900 was supplied by Nisso Chemical Europe GmbH (NCE, Düsseldorf, Germany). Glycerol, sodium chloride, trichlorooctadecylsilane (TCI) and 2,2,4-trimethylpentane were purchased from Aladdin Chemical Co. (Shanghai, China). PDMS and Sylgard 184 were supplied by Dow Corning Co., Ltd. (Midland, United States). PDMS films (KYN-100 μ m) were obtained from Bald Advanced Materials Company (Hangzhou, China). Translucent polyester film was purchased from Shunhe Packing Co., Ltd (Guangdong, China). Silicon wafers of *ca.* 10 cm diameter and 1 mm thickness were supplied by Jiutao Sensor Technology Co., Ltd (Suzhou, China) and AZP4620 as the photoresist by Shenzhen QY Opto-Electronics (Shenzhen, China).

Fabrication of stretchable PDMS molds

After DRIE etching, the positive-acting photoresist was removed by oxygen plasma etching and the micropatterned wafer was soaked in 1 mM TCI dissolved in 2,2,4-trimethylpentane for 30 min. PDMS and the curing agent Sylgard 184 (at a mass ratio of 12:1) mixed with black dye (Cannon, Japan) was poured into a petri dish with the

inverted superhydrophobic wafer pressed on the surface and two PET films (500 μm - 2 mm) as the thickness gage. The mixture was placed in a vacuum container to remove air bubbles and kept at room temperature (25 $^{\circ}\text{C}$) for 72 h for solidification. Silver wire was embedded in the groove before solidification, and the resulting PDMS molds were treated with O_2 plasma.

Characterization

The morphology and elemental mapping of HPC LCs were characterized by a SU8010 microscope (Hitachi, Japan) after sputtering the samples with a thin gold layer (Emitech, K550). The contact angles (CAs) of HPC/ H_2O /Gly liquids (15 wt% HPC and 0-18 wt% Gly relative to HPC) were determined on an OCA 100 contact angle test system (DataPhysics, Germany) using 5 μL of liquid each time. Reflectance spectra were collected by an 7-channel spectrometer (Avantes, AvaSpec-ULS2048CL, holland) with an in-situ fiber optic probe. Stereomicroscopy was carried out using a Keyence VHX-1000 digital microscope (Osaka, Japan). A rheometer (ARES-G2, TA Instruments, Delaware, USA) equipped with a parallel-plate fixture (25 mm in diameter) was used to study the dynamic rheological behavior of HPC LC at a heating rate of $1^{\circ}\text{C min}^{-1}$.

The voltage and charge quantity were recorded by an electrometer (Huace EST102, Beijing, China) with the force applied by different weights. To demonstrate a wearable self-charging powered package, the overlapping-joint-structure HPC-based LC-TENG was used to charge a commercial capacitor (2.2 μF) through a bridge rectifier. The voltage changes in these capacitors were discharged by connecting to a resistor and measured using a digital source meter (Fluke 8846A, Shanghai, China).

Finite Element Method (FIM) was employed to simulate the processes such as water evaporation, mechanical deformation and electric field distribution using COMSOL Multiphysics.

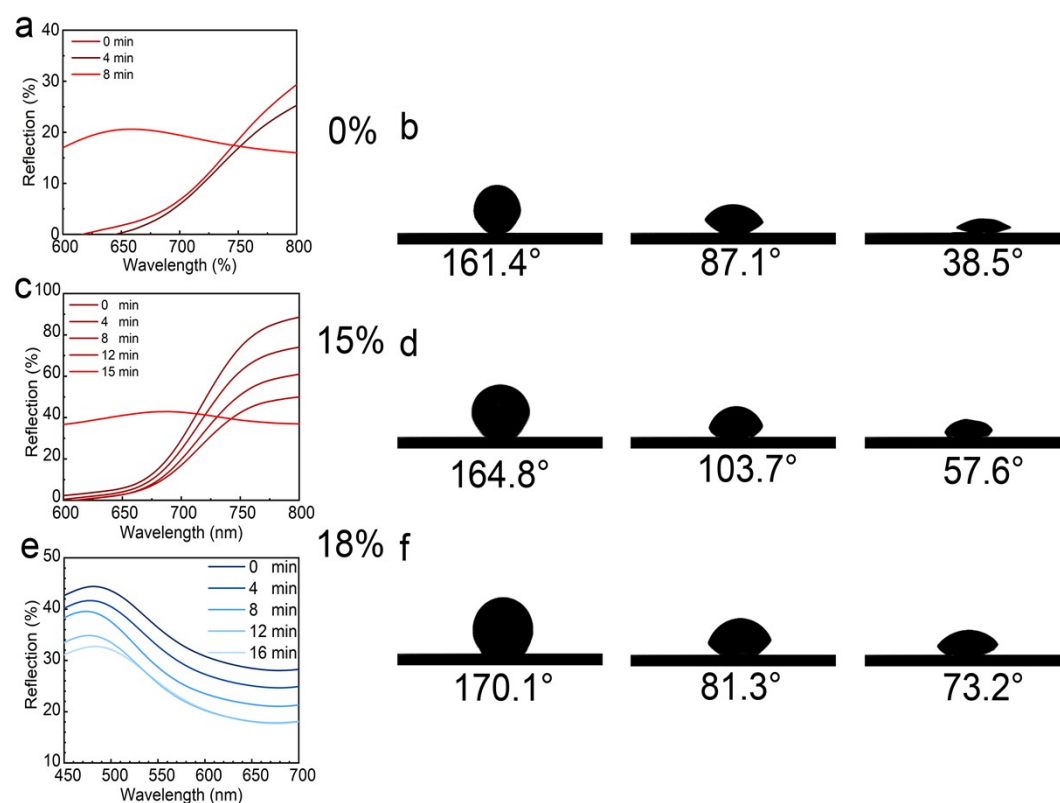


Figure S1. a, c, e) The tuning of the structural color of the HPC/Gly/ion LC with different glycerol contents (0-18 wt% relative to HPC). b, d, f) Corresponding contact angles (CAs) of the LC precursor droplets measured on a PDMS substrate as a function of time.

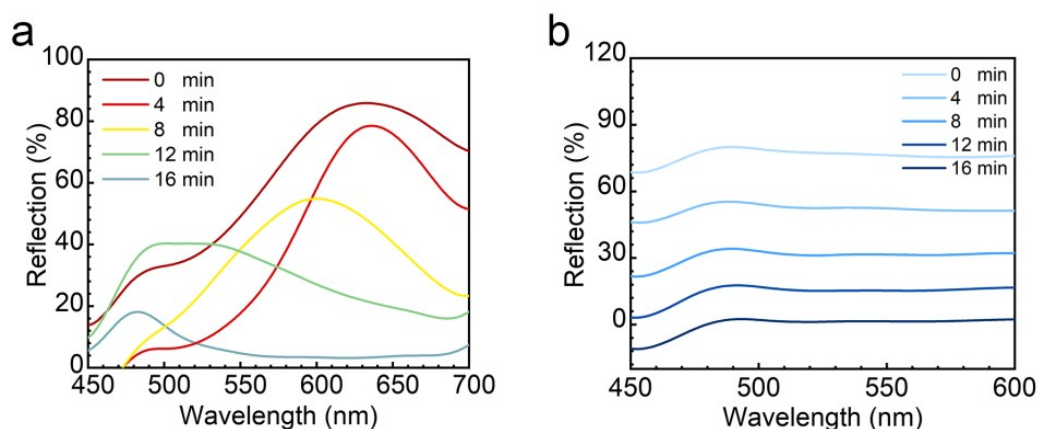


Figure S2. The tuning of the structural color of the HPC/polyol/ion LC with a) 15 wt% glycol or b) 5 wt% sorbitol.

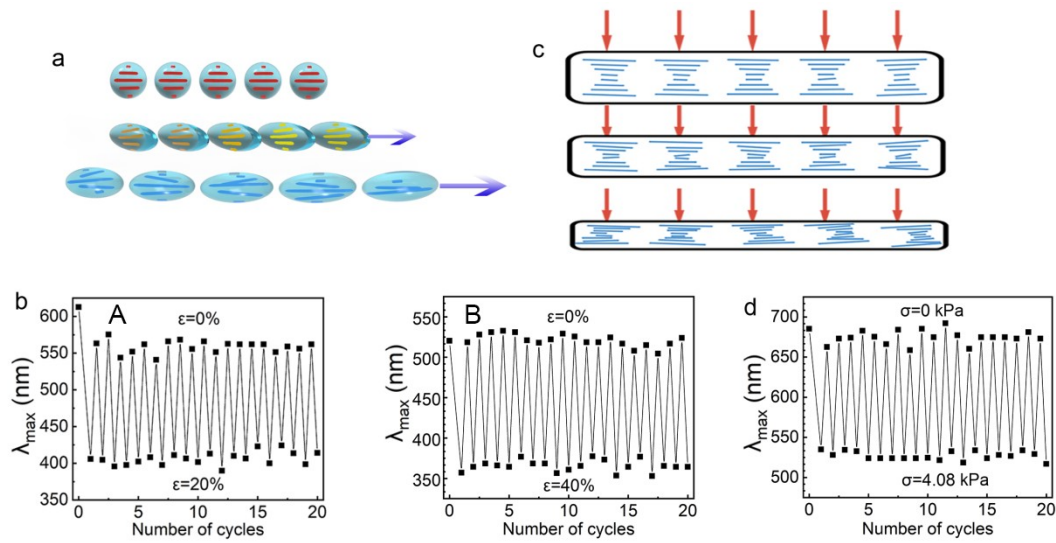


Figure S3. a) Schematic representation of the changes of helicoidal domains and b) Change of λ_{\max} during stretching. c) Schematic representation and d) Change of λ_{\max} during compression.

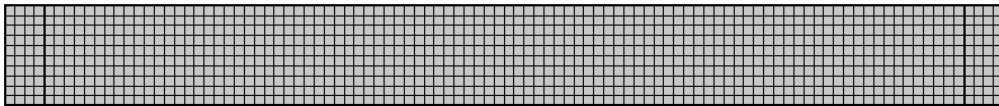


Figure S4. Grids in the LC stripe used for tensile deformation behavior algorithms.

Colors recorded by the camera consist of three 8-bits values for the three primary channels R (red), G (green) and B (blue). R is set as (255, 0, 0), G is set as (0, 255, 0) and B is set as (0, 0, 255). A color diagram with coordinates r on the red channel, g on the green channel and b on the blue channel is represented by (r, g, b) in RGB coordinates, given by $r R + g G + b B$. On the RGB triangle plot, R, G and B vectors are set at a radius equal to 1 and at an angle of 120° from each other (the red, green and blue diamonds and lines), to make an equal re- partition.

$$x_R=1$$

$$y_R=0$$

$$x_G=\cos(120^\circ)$$

$$y_G=\sin(120^\circ)$$

$$x_B=-\cos(120^\circ)$$

$$y_B=-\sin(120^\circ)$$

$$\alpha=r \times x_R + g \times x_G + b \times x_B / r + g + b$$

$$\beta=r \times y_R + g \times y_G + b \times y_B / r + g + b$$

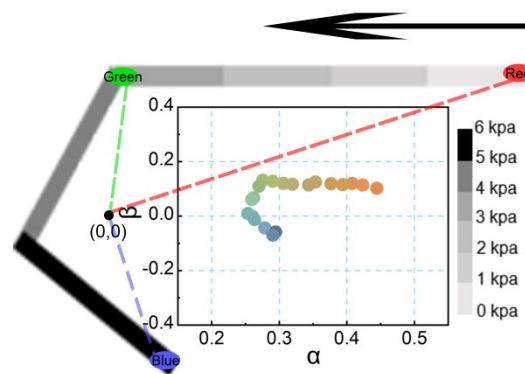


Figure S5. Ternary diagrams with primary color axes, which was calculated using the above equations.

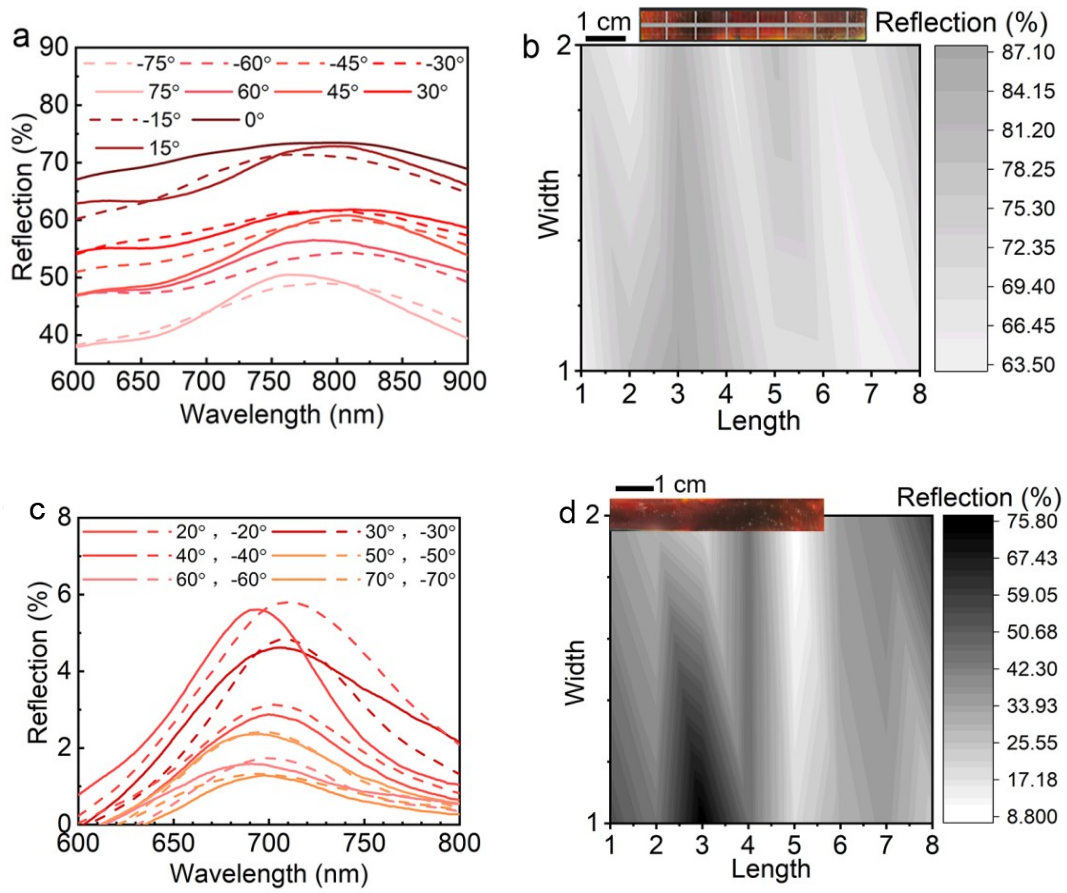


Figure S6. a, c) Reflectance spectra and b, d) reflected intensity distribution of the a, b) HPC/Gly/ion and c, d) HPC/ion sensors.

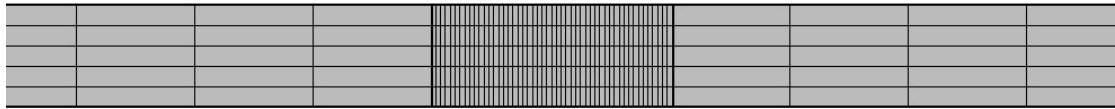


Figure S7. Grids in the LC stripe used for compressive stress transferring behavior algorithms.

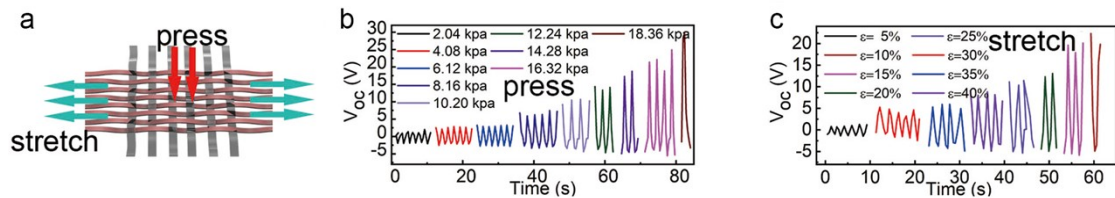


Figure S8. a) Schematic diagram and electrical output during b) compressing and c) stretching tests

(sample: ca. 5 cm \times 4 cm).

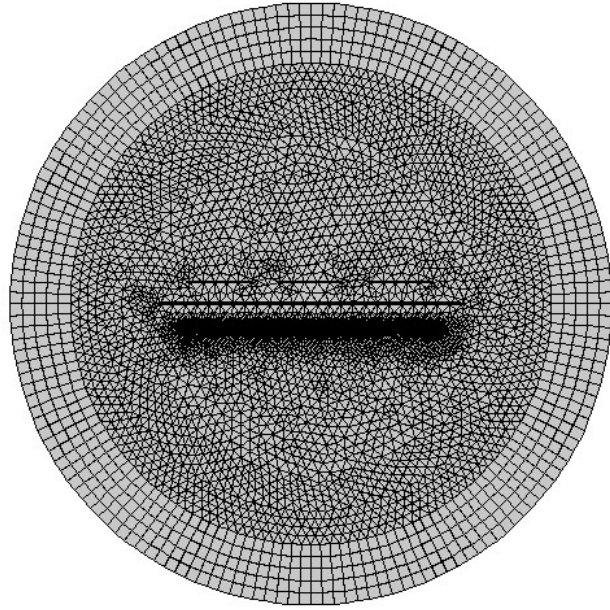


Figure S9. Grids in the LC-TENG device using for electric field distribution algorithms.

Electricity generating process

To obtain a more quantitative understanding of the electricity generating process, we establish a corresponding theoretical electric potential distribution model between the polyester films and the LC-PDMS unit by a simple finite element simulation using COMSOL Multiphysics (Figure 6 and Figure S9). Due to contact-electrification effect, charges will be transferred between PDMS and polyester layers. When these two materials are in full contact, the whole device is electric neutral (Figure 6f-I, g-I). When the two materials are separated, the positive charges in the LC gel move near the PDMS film to maintain the electrostatic balance of the LC-PDMS unit (Figure 6f-II, g-II). In the meantime, the LC gel near the silver wire is negatively charged, resulting in a electron current from the wire to the ground. When the distance between PDMS and polyester exceeds a certain value, no current flows between the LC gel and the ground due to the new-formed charge balance (Figure 6f-III, g-III). When PDMS contacts the polyester again, the positive charges in the LC move from near the PDMS to near the wire underneath (Figure 6f-IV, g-IV).